Electron spin resonance of $YbIr_2Si_2$ below the Kondo temperature

2007 J. Phys.: Condens. Matter 19 016211

(http://iopscience.iop.org/0953-8984/19/1/016211)

INSTITUTE OF PHYSICS PUBLISHING JOURNAL OF PHYSICS: CONDENSED MATTER

J. Phys.: Condens. Matter **19** (2007) 016211 (6pp) doi:10.1088/0953-8984/19/1/016211

Electron spin resonance of $YbIr_2Si_2$ below the Kondo temperature

J Sichelschmidt[1], J Wykhoff[1], H-A Krug von Nidda[2], I I Fazlishanov[1,2,3], Z Hossain[1], C Krellner[1], C Geibel[1] and F Steglich[1]

[1] Max Planck Institute for Chemical Physics of Solids, 01187 Dresden, Germany
[2] Experimentalphysik V, EKM, Universität Augsburg, 86135 Augsburg, Germany
[3] E K Zavoisky Physical-Technical Institute, 420049 Kazan, Russia

E-mail: Sichelschmidt@cpfs.mpg.de

Received 4 September 2006, in final form 18 October 2006
Published 7 December 2006
Online at stacks.iop.org/JPhysCM/19/016211

Abstract

We report an electron spin resonance (ESR) study in single crystals of the new heavy-fermion metal $YbIr_2Si_2$ whose spin dynamics is characterized by a Kondo energy scale $T_K \simeq 40$ K and which acquires a Landau Fermi-liquid state below 0.2 K. The ESR spectra are observed well below T_K and show typical properties of a Yb^{3+} resonance. This enables the direct observation of the spin dynamics and static magnetic properties of $YbIr_2Si_2$ below the Kondo temperature.

(Some figures in this article are in colour only in the electronic version)

1. Introduction

The heavy-fermion metal $YbIr_2Si_2$ is the first example of an Yb system close to a zero-temperature quantum phase transition (QPT) which is located on the non-magnetic side, i.e., a Landau Fermi-liquid state is reached below 0.2 K [1]. $YbIr_2Si_2$ is expected to be close to a magnetic instability, related to the appearance of antiferromagnetic (AF) order (due to decreasing 4f–conduction electron hybridization) when external pressure is applied. The body-centred, I-type $YbIr_2Si_2$ is structurally homologous to $YbRh_2Si_2$ which has attracted considerable attention in recent years due to its proximity to a magnetic field-induced quantum critical point [2, 3]. The electrical resistivity, specific heat, and magnetic susceptibility of $YbIr_2Si_2$ show typical Kondo lattice behaviour. The magnetic entropy reaches $0.5R\ln 2$ at 20 K, from which a Kondo temperature $T_K \simeq 40$ K can be estimated [1].

$YbRh_2Si_2$ is the first dense Kondo system in which a narrow, well-defined electron spin resonance (ESR) line could be detected well *below* $T_K \simeq 20$ K [4], down to at least 0.6 K. Although the exact origin of this ESR signal is yet unclear, key properties like the ESR g-factor and its anisotropy clearly reflect characteristics of the Kondo ion Yb^{3+} itself [5]. On the

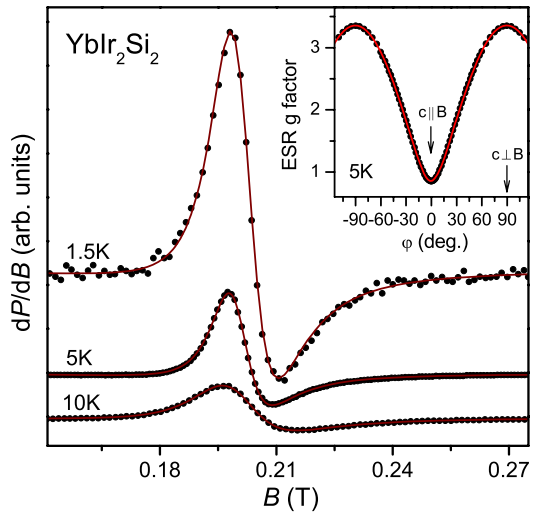

Figure 1. ESR spectra at 9.4 GHz (X-band) at selected temperatures. Solid lines represent fits to the data with a Lorentzian line shape showing an asymmetry typical for metals. Inset: anisotropy of the ESR g-factor at $T = 5$ K. The tetragonal c-axis encloses the angle φ with the magnetic field B-direction. The solid line fits the data with a uniaxial symmetry behaviour; see text.

other hand, in order to investigate the Kondo ion spin dynamics of Ce-related heavy-fermion compounds one was forced to use diluted paramagnetic probe spins at the Ce site, Gd in most cases [6]. Therefore, the ESR as observed in $YbRh_2Si_2$ has proven to be a unique tool for *directly* characterizing the Kondo ion spin dynamics. Here, we report the second example of an Yb-based heavy-fermion metal in which an ESR is observable well below T_K without doping ESR probe spins.

2. Experiment and results

The preparation as well as the magnetic and transport properties of $YbIr_2Si_2$ have been described elsewhere [1]. Depending on the preparation conditions, $YbIr_2Si_2$ crystallizes in two different structures, either in the primitive tetragonal (P) type or in the body-centred tetragonal (I) type [1]. The local crystal-field symmetry of the Yb site differs profoundly in both structure types of $YbIr_2Si_2$, although they both have almost the same lattice parameters. The P-type crystals acquire a much lower residual resistivity ratio, $\rho_{300\,K}/\rho_0 \sim 2$, than that of the I-type crystals, $\rho_{300\,K}/\rho_0 > 200$. The latter value evidences little crystalline disorder and a high quality of the I-type single crystals.

The ESR measurements were performed at a frequency of 9.4 GHz at temperatures 1.5 K $\lesssim T \lesssim$ 30 K. We investigated four single-crystalline platelets of I-type $YbIr_2Si_2$ of two batches (thickness $\lesssim$250 μm, $\lesssim$4 mm^2 surface area) and four P-type samples from two batches. Electron microprobe analysis confirms the surface composition to be $YbIr_2Si_2$ with less than 1% of spurious phases. Experimentally, ESR is observed by measuring the absorbed power P of a transversal magnetic microwave field as a function of an external, static magnetic field B. Figure 1 shows typical spectra of I-type $YbIr_2Si_2$ which are recorded as dP/dB versus B. As previously found in the $YbRh_2Si_2$ system, no hyperfine structure which may arise due to ^{171}Yb and ^{173}Yb was observable in the whole temperature region, likely due to the mechanism of a strong exchange narrowing of the ESR line. No ESR line of P-type $YbIr_2Si_2$ was observed

in the temperature region 2–300 K. We attribute this absence to the much lower Kondo scale $T_K \sim 2$ K and the concomitant more stable magnetically ordered state in the P-type $YbIr_2Si_2$ (magnetic order below $T = 0.7$ K) compared to the I-type $YbIr_2Si_2$. We found no indications of a broad line which could result from broadening due to the larger crystalline disorder in the P-type samples.

The asymmetry of the line shape is due to a non-vanishing dispersion contribution to the line and is typical for metallic samples [7]. As shown by the solid line in figure 1, the experimental line shape excellently agrees with a metallic Lorentzian. Within experimental uncertainties the ratio of dispersion to absorption in the resonance line was found to be close to one and constant throughout the whole temperature range investigated. This behaviour is expected if the sample size exceeds the microwave penetration depth [7], which for our crystals varies from $\approx$0.4 μm at $T = 1.5$ K to $\approx$2.6 μm at $T = 25$ K. This finding already indicates an at most minor influence of the sample surface to the ESR signal. Moreover, the ESR line parameters of all four I-type $YbIr_2Si_2$ samples investigated show exact agreement.

An ESR signal arising from the bulk of the $YbIr_2Si_2$ crystals should reflect their highly anisotropic magnetic susceptibility [1]. Indeed, the ESR g-factor (as determined by the resonance condition $h\nu = g\ \mu_B B_{Res}$) shows a correspondingly large anisotropy. The inset of figure 1 shows $g(\varphi)$ when the crystalline c-axis is rotated by angle φ with respect to the direction of B, and when the microwave magnetic field is kept in the tetragonal basal plane. The solid line describes the data with a uniaxial symmetry behaviour: $g(\varphi) = \sqrt{g_\parallel^2 \cos^2\varphi + g_\perp^2 \sin^2\varphi}$. At $T = 5$ K: $g_\parallel(5\text{ K}) = 0.85 \pm 0.01$, $g_\perp(5\text{ K}) = 3.357 \pm 0.005$. Clearly, demagnetization effects could not cause such a pronounced anisotropy. For our platelet-shaped crystals with the c-axis oriented perpendicular to the platelet surface, estimations of the demagnetizing field according to [8] (equation (7)) yield a 0.5% upward shift of $g_\perp(5\text{ K})$. Compared with $YbRh_2Si_2$ [4] the ESR g-factor is less anisotropic, in agreement with the smaller anisotropy of the magnetic susceptibility. We analysed the symmetries Γ_6 or Γ_7 which characterize the wavefunctions of the two lowest Kramers doublets of the Yb^{3+} ground state in a tetragonal environment. Whereas in $YbRh_2Si_2$ the Γ_7 ground state symmetry corresponds to g-factors which are closer to the measured ones [5], in $YbIr_2Si_2$ both Γ_6 or Γ_7 would describe the experimental g-factors with a g-shift $\Delta g \approx -5\%$. This g-shift means a shift of the g-factor respective to its value in an ionic, insulating environment. In the case of an isothermal ESR in metals $\Delta g \propto N(\epsilon_F)J(q = 0)$, where $N(\epsilon_F)$ is the density of states at the Fermi energy and $J(q)$ is the local moment–conduction electron exchange integral at wavevector $\mathbf{q} = 0$ [7].

The nature of the relaxation mechanism of the ESR-active spins is reflected by the linewidth ΔB which is measured as the half width at half maximum of $P(B)$. Its T-dependence is shown in figure 2 for two orientations of the crystal in the magnetic field, $B \perp c$-axis and $B \parallel c$-axis. The dashed line displays the behaviour which is typical for local moment relaxation in a metallic environment [7, 9]: $\Delta B(T) = \Delta B_0 + bT + \frac{c\Delta}{\exp(\Delta/T-1)}$. The linewidth data for $B \perp c$ are well described with $\Delta B_0 = 7$ mT, $b = 0.5$ mT K^{-1}, $c = 17$ mT K^{-1}, and $\Delta = 60$ K. It is noteworthy that, in contrast to the data for $YbRh_2Si_2$, the linear temperature dependence of $\Delta B(T)$ is almost invisible. Therefore, assuming a isothermal local moment relaxation in a metallic environment to cause typically a linear slope b (the Korringa slope, [7]), the ESR relaxation in $YbIr_2Si_2$ seems to contain only small contributions from conduction electrons (CEs). A reduced Korringa slope behaviour was also found for the ESR of diluted Yb^{3+} in the intermediate valence system $CePd_3$ [9] which could be explained by a reduced CE density of states around the Fermi energy. Similar to $YbRh_2Si_2$, above $T \simeq 10$ K an exponential increase of $\Delta B(T)$ dominates. We attribute this behaviour to the first excited crystal-field states

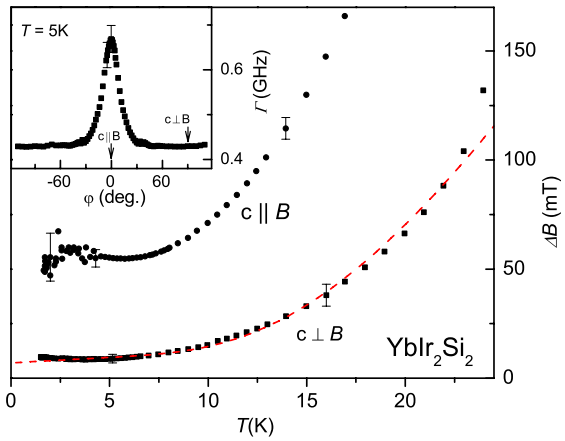

Figure 2. Temperature dependence of the ESR linewidth ΔB of $YbIr_2Si_2$ at two orientations of the crystalline c-axis in the magnetic field. The dashed line represents the data as explained in the text. The inset shows the angular dependence of the relaxation rate Γ.

which contribute to the relaxation with increasing temperature [7]. Inelastic neutron scattering experiments yield crystalline electric-field transition energies of 18, 25, and 36 meV [10], very similar to those of $YbRh_2Si_2$ (17, 25, 43 meV) [11]. However, comparing for both compounds the parameters of the exponential increase of $\Delta B(T)$, considerably smaller values are found in $YbIr_2Si_2$. In $YbRh_2Si_2$ the values are $c = 100$ mT K^{-1}, and $\Delta = 115$ K. In $YbIr_2Si_2$, like the linear slope b, the reduced values c and Δ could reflect a reduced contribution of conduction electrons to the relaxation mechanism. Towards the low-temperature end the linewidth data tend to approach a saturation value. The $c \parallel B$ data show a slight tendency to decrease below $T = 3$ K. For $T \gtrsim 25$ K the ESR signal is too weak and too broad to be detected.

As shown in the inset of figure 2, a pronounced anisotropy of the relaxation rate $\Gamma = g\ \mu_B \Delta B/h$ is observed when approaching the $c \parallel B$ orientation. The microwave magnetic field was aligned perpendicular to the c-axis. Again, very similar behaviour was found in $YbRh_2Si_2$ [5]. There the anisotropy of Γ was shown to be caused by the anisotropy of the residual relaxation rate, i.e. the zero-temperature linewidth anisotropy (obtained from extrapolating the Korringa slope of $\Delta B(T)$ to zero temperature) [5]. The temperature dependence of the ESR g-factor is shown in figure 3 for the two crystal orientations $c \perp B$ and $c \parallel B$. At temperatures above 15 K a slight decrease with increasing temperature is notable for the $c \perp B$ orientation. This behaviour indicates a temperature-dependent g-shift due to the influence of the first excited crystalline-field levels. As can be seen in the inset of figure 3, the latter behaviour is more pronounced in $YbRh_2Si_2$. Towards low temperatures the g-factor temperature dependence of $YbIr_2Si_2$ differs from that of $YbRh_2Si_2$. When comparing the $g_\perp$ data, instead of a strong downturn in $YbRh_2Si_2$ (inset figure 3) in $YbIr_2Si_2$ a slight upturn is observed. Note that the latter behaviour may readily be explained by demagnetization effects as estimated above. We could not compare the corresponding $g_\parallel$ data because of missing corresponding data for $YbRh_2Si_2$. It is worth mentioning that the temperature dependence of the ESR g-factor in $YbIr_2Si_2$ is different for the two crystal orientations $c \perp B$ and $c \parallel B$. Such behaviour is typical for an anisotropic bottleneck ESR in metallic environments as has for instance been observed in the high-temperature superconductor $La_{2-x}Sr_xCuO_4$ [12].

The ESR intensity I_{ESR} which corresponds to the uniform magnetic susceptibility of the probed ESR spin is shown in figure 4. I_{ESR} is proportional to the integral of the absorption

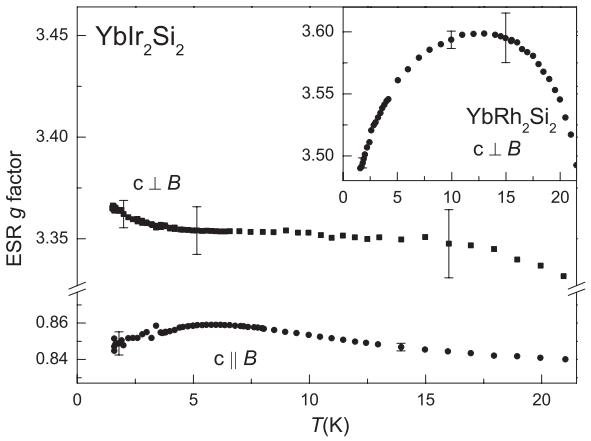

Figure 3. Temperature dependence of the ESR g-factor of $YbIr_2Si_2$ at two orientations of the crystalline c-axis in the magnetic field. Inset: g-factor data for $YbRh_2Si_2$ at $c \perp B$. Note the qualitative difference from $YbIr_2Si_2$ in the temperature behaviour towards low temperatures.

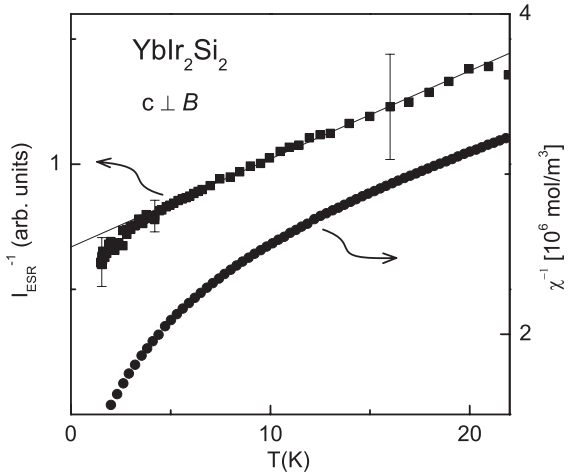

Figure 4. Comparison of the temperature dependences of the reciprocal ESR intensity I_{ESR}^{-1} (squares, left axis) and reciprocal static magnetic susceptibility χ^{-1} (circles, right axis). The solid line shows a Curie–Weiss law $(T - \Theta)$, $\Theta = -20$ K.

line which has been determined by $I_{\mathrm{ESR}} \propto A\Delta B^2$ (where A denotes the signal amplitude). For a proper calculation of $I_{\mathrm{ESR}}(T)$ we took the normal skin effect into account. We divided $A\Delta B^2$ by the temperature-dependent microwave penetration depth, which is determined by the electrical conductivity (see [1]). For $T > 5$ K, I_{ESR} follows nicely a Curie–Weiss law with a negative Weiss temperature of $\Theta_\perp = \Theta_\parallel = -20$ K, indicating AF correlations. Below $T \approx 5$ K, I_{ESR}^{-1} starts to deviate from a linear temperature dependence. As can be seen in figure 4, this behaviour qualitatively resembles the temperature dependence of the bulk susceptibility which we measured at the same crystal and at $B = 0.2$ T, which is the resonance magnetic field. This indicates that the measured ESR signal corresponds to a bulk property of $YbIr_2Si_2$.

3. Conclusion

We have reported an EPR signal in single crystals of the heavy-fermion metal $YbIr_2Si_2$ (I-type structure). As in the case of the ESR in $YbRh_2Si_2$, the signal shows up *below* the single-ion Kondo temperature $T_K = 40$ K. It shows clear characteristics of a Yb^{3+} spin whose local character is displayed in the Curie–Weiss-like temperature behaviour of the ESR intensity. From the anisotropy of the ESR g-factor both Γ_6 and Γ_7 symmetries of the crystal-field-derived Kramers doublet are possible. Unlike the case of $YbRh_2Si_2$ in $YbIr_2Si_2$, the temperature dependence of the ESR linewidth does not show a Korringa slope, suggesting that the contribution of conduction electrons to the relaxation is very weak. The temperature dependence of the ESR g-factor is different for the two crystal orientations $c \perp B$ and $c \parallel B$, which is typical for anisotropic bottleneck ESR in metallic environments.

Acknowledgments

The low-temperature ESR-measurements at the University of Augsburg were partially supported by the German BMBF under Contract No. VDI/EKM13N6917 and by the Deutsche Forschungsgemeinschaft within SFB484 (Augsburg).

References

[1] Hossain Z, Geibel C, Weickert F, Radu T, Tokiwa Y, Jeevan H, Gegenwart P and Steglich F 2005 *Phys. Rev.* B **72** 094411
[2] Gegenwart P, Custers J, Geibel C, Neumaier K, Tayama T, Tenya K, Trovarelli O and Steglich F 2002 *Phys. Rev. Lett.* **89** 056402
[3] Custers J, Gegenwart P, Wilhelm H, Neumaier K, Tokiwa Y, Trovarelli O, Geibel C, Steglich F, Pépin C and Coleman P 2003 *Nature* **424** 524–7
[4] Sichelschmidt J, Ivanshin V A, Ferstl J, Geibel C and Steglich F 2003 *Phys. Rev. Lett.* **91** 156401
[5] Sichelschmidt J, Wykhoff J, Krug von Nidda H-A, Ferstl J, Geibel C and Steglich F 2006 *Preprint* cond-mat/0609020
[6] Krug von Nidda H-A, Heinrich M and Loidl A 2003 *Relaxation Phenomena* ed W Haase and S Wróbel (Berlin: Springer) pp 112–35
[7] Barnes S E 1981 *Adv. Phys.* **30** 801–938
[8] Deisenhofer J, Krug von Nidda H-A, Loidl A, Ahn K, Kremer R K and Simon A 2004 *Phys. Rev.* B **69** 104407
[9] Gambke T, Elschner B, Kremer R and Schanz M 1983 *J. Magn. Magn. Mater.* **36** 115–24
[10] Hiess A, Stockert O, Koza M M, Hossain Z and Geibel C 2006 *Physica* B **378–380** 748–9
[11] Stockert O, Koza M M, Ferstl J, Murani A P, Geibel C and Steglich F 2006 *Physica* B **378–380** 157–8
[12] Kochelaev B I, Sichelschmidt J, Elschner B, Lemor W and Loidl A 1997 *Phys. Rev. Lett.* **79** 4274–7